RSC Advances

This article can be cited before page numbers have been issued, to do this please use: R. nouri, S. Abedi and A. Morsali, *RSC Adv.*, 2016, DOI: 10.1039/C6RA23075J.

ROYAL SOCIETY OF CHEMISTRY

www.rsc.org/advances

View Article Online
DOI: 10.1039/C6RA23075J

Journal Name

ARTICLE

Design and synthesis of two novel functional metal-organic microcapsules, an investigation on ligand expansion effects on metal-organic microcapsules' properties

Received 00th January 20xx,
Accepted 00th January 20xx

DOI: 10.1039/x0xx00000x

www.rsc.org/

R. Nouri, S. Abedi, A. Morsali*

In this study, two novel metal-organic capsules were synthesized based on coordination-directed organization of two new extended tetrazolate ligands (1,4-bis((1H-tetrazol-5-yl)methyl)benzene (btmbenzene), 4,4'-bis((1H-tetrazol-5-yl)methyl)biphenyl (btmbiphenyl)) and Zn^{2+} ions. Furthemore, functions of these capsules in inclusion of inorganic nanoparticles (Fe_3O_4), dye (Rhodamine B) and drug (5-fluorouracil) were investigated. Moreover, effects of ligand expansion on the size, morphology, loading capacity and other properties of these capsules were studied. In addition, other morphologies of these coordination polymers in different conditions were fabricated. Finally, obtained microcapsules were utilized for synthesis of crystalline ZnO hollow spheres via calcination method.

Introduction

Infinite coordination polymers (ICPs) consist of polymerized metal-ligand networks which can be synthesized by self-assembly of metal nodes and a polydentate organic ligand, have recently been regarded as a captivating innovative class of inorganic–organic materials.[1-3] Metal–organic capsules with capability of adaptive entrapment of various functional species are new ICP materials which have appealed to researchers in recent years. Newly, various guest materials as exemplified by drugs, dyes, small nanoparticles, nucleotides, have been included into self-supported ICPs coordination networks.[4,5,7,8,9,10,11] In 2009, Kimizuka *et al.* reported preparation of supramolecular networks constructed from lanthanide ions and nucleotides which exhibited adaptive encapsulation features. Moreover, ability of these capsules as contrast enhancing agents for magnetic resonance imaging (MRI) were proved.[5] However, the main drawback of lanthanide-containing compounds is their toxicity toward the living systems.[6] Concurrently, inorganic-organic empty spheres consisting of Zn(II) metal ions and 1,4-bis(imidazol-1-ylmethyl) benzene (bix) were synthesized based on the self-assembly technology by Maspoch *et al*..[4] Significance of these capsules was in their magnitude which scope in dimension from about 100 nm to over 1 µm. These capsules are bigger than metal–organic polyhedra that commonly have sizes of a few nanometers with narrow ability of inclusion of small numbers of guest molecules.[7,8] Afterward in 2010, discus-like nanoscale coordination polymers comprising a π-conjugated dicarboxylate ligand and lanthanide ions were fabricated by Uvdal *et al.* which demonstrated guest inclusion properties. Interestingly, loading quantity of guest molecules into these ICPs can be regulated by altering synthesis temperatures.[9] Next, Mao and coworkers could prepare ICP nanoparticles from b-nicotinamide adenine dinucleotide and terbium ions with encapsulation ability.[10] In 2014, our group revealed synthesis of ICP nanocapsules assembled from the metal node (Zn^{2+}) and ditopic organic ligand (btb: 1, 3-bis(tetrazol-5-ylmethyl)benzene) Zn(btb) with spherical morphology. Accordingly, some core-shell particles could also be synthesized via calcination of tetrazole-based ICP capsules.[11] Recently reported metal-organic capsules with ability of confining inorganic particles belong to Zhang et al. which were prepared via photodecomposition of ferrocenedicarboxylic acid in methanol.[12] A dominant challenge in the fabrication of functional metal-organic capsules is to change chemical components and increase host-guest interactions without transforming the fundamental morphology. Expansion is a regular aspect of metal-organic frameworks (MOFs) fabrication and directional-bonding synthesis of supramolecular coordination compounds.[13] Generally in this method, ligands with additional phenyl or ethynyl groups are applied that raise the length between Lewis basic centers of a polydentate linker.[13] Addition of phenyl or ethynyl spacers leads to enlargement of the dimension of MOFs cavities and internal pores of supramolecular coordination compounds without important influence on the synthesis route. Applying expanded linkers with a specific secondary building unit (SBU) results in fabrication of a series of analogous MOFs which have the same network topology.[13] Effects of adding a phenyl group on the size and other properties of metal-organic capsules have not been investigated yet.

Department of Chemistry, Faculty of Sciences, Tarbiat Modares University, P.O. Box 14115-4838, Tehran, Iran. E-mail: morsali_a@modares.ac.ir; Fax: +98 21 8009730; Tel: +98 21 82884416

† Footnotes relating to the title and/or authors should appear here.
Electronic Supplementary Information (ESI) available: [details of any supplementary information available should be included here]. See DOI: 10.1039/x0xx00000x

View Article Online
DOI: 10.1039/C6RA23075J

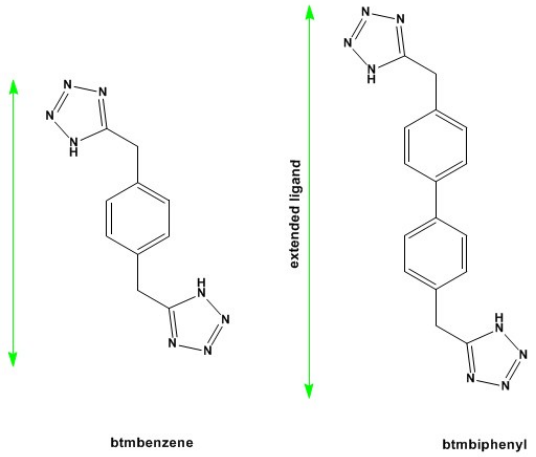

Scheme 1 N-donor-based building blocks for this project.

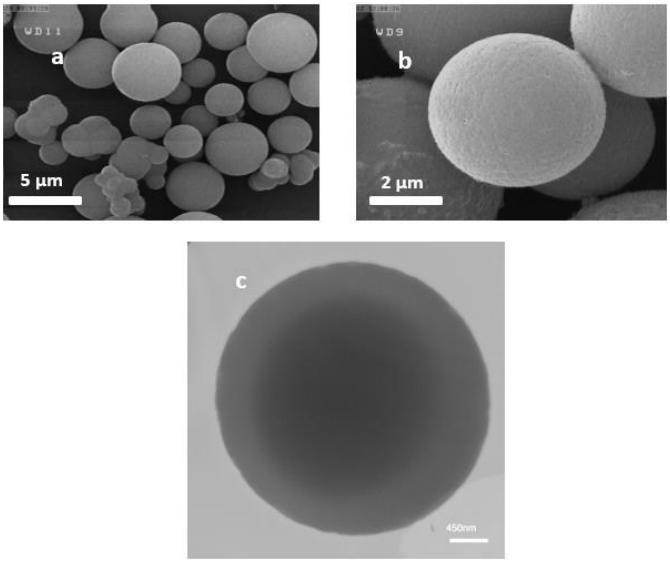

Fig. 1 a) Low-magnification SEM images of the Zn(btmbenzene)-1 spheres. b) High-magnification SEM image. (c) High-resolution TEM image of an individual Zn(btmbenzene)-1 sphere.

We supposed that addition of a phenyl group would result in the larger dimensions of the metal–organic spheres and the prepared capsules could entrap more amounts of the guest molecules.[13] Moreover, additional phenyl ring in the linker leads to an increase in the electron density of the structure and favorable π-π interactions. Hence, such capsules could have a better interaction with guest molecules.[14] Therefore, we aimed to design two novel metal-organic ICP capsules based on two new tetrazolate ligands of different length to investigate expansion effects on these materials (Scheme 1). Moreover, other morphologies of these coordination polymers were synthesized in different conditions. We hope that this work can open a new route for the synthesis of various tetrazole-based metal-organic microcapsules with novel extended linkers of the same type and maintaining the original morphology.

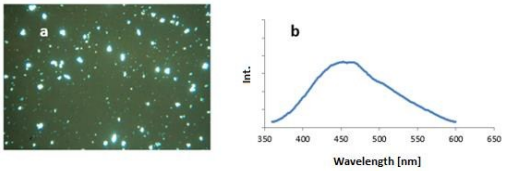

Fig. 2 a) Fluorescence microscopy image of Zn(btmbenzene)-1 microspheres deposited onto glass (λ_{ex}=359–371 nm, λ_{em}> 440 nm) b) PL spectrum collected at λ_{exc}=350 nm.

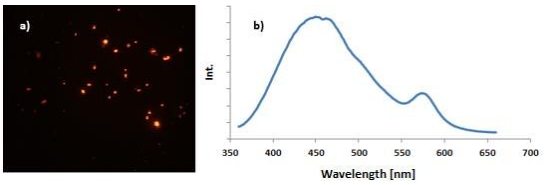

Fig. 3 Fluorescence optical microscopy images of (a) RhB@Zn(btmbenzene)-1 (λ_{exc}=540–552 nm, λ_{em}> 590 nm) b) PL spectrum collected at λ_{exc}= 350 nm.

Results and Discussion

All ligand syntheses were carried out under an argon atmosphere by reacting the corresponding 2,2'-(1,4-phenylene)diacetonitrile and 2,2'-(biphenyl-4,4'-diyl)diacetonitrile with sodium azide and triethylamine hydrochloride in accordance with literature procedures (ESI).[15] To prepare btmbenze ligand, 2,2'-(1,4-phenylene)diacetonitrile, sodium azide and triethylamine hydrochloride were refluxed in dry toluene for 72 h under an inert argon atmosphere. The work up was performed according to detailed information available in electronic supplementary information (ESI). The prepared product was characterized by ^{1}H NMR, ^{13}C NMR spectroscopy (Fig. S2 and Fig. S3 respectively†) and elemental analysis. All analyses confirmed the formation of btmbenzene ligand. In an experiment, methanolic solution of $Zn(NO_3)_2.6H_2O$ was added to the DMF solution of tetrazolate ligand (btmbenzene, Scheme 1) under stirring and the homogenized mixture poured into a Teflon-lined stainless steel autoclave. Subsequently, it was heated at 120 °C for 12 h and then cooled to room temperature for 3 h which ended up preparing white powder named as Zn(btmbenzene)-1. To purify the product, the mixture was washed with DMF several times and centrifuged. Field-emission scanning electron microscopy analysis of Zn(btmbenzene)-1 showed that the product consists of spheres with average diameters of 5 µm which have smooth surfaces. Fig. 1 (a and b) shows SEM images of bare Zn(btmbenzene)-1 microspheres. Fig. 1 (c) demonstrates corresponding high resolution transition electron microscopy (HRTEM) image of the Zn(btmbenzene)-1 which confirms these microcapsules are hollow. FT-IR spectrum of the compound displayed two strong peaks in 1431 and 1657 cm^{-1} which are attributed to deprotonation of tetrazole rings and coordination of ditopic ligands to Zn^{2+} cations (Fig. S7†). Thermogravimetric analysis (TGA) of ICPs were performed at a range from 25-800 °C under a flow of nitrogen gas at a constant rate of 10 °C/min to investigate the weight loss as a function of temperature and evaluate the thermal stability.

Scheme 2 Synthesis of btmbenzene-based micro- and nano-structures: (a) MeOH/DMF/solvothermal conditions (b) MeOH/DMF/fast precipitation method, (c) H_2O/DMF/reflux, (d) H_2O/DMF/solvothermal.

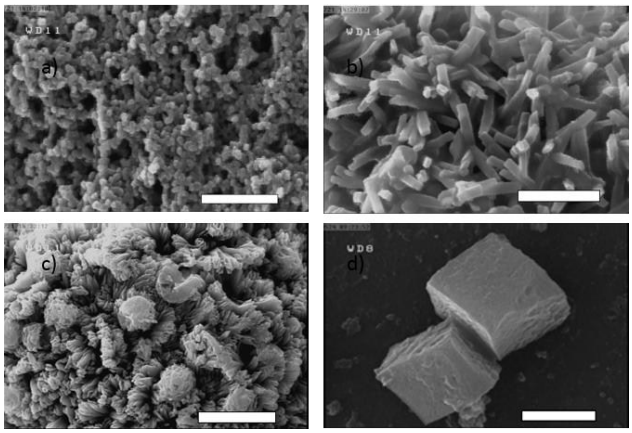

Fig. 4 SEM images of (a) Zn(btmbenzene)-2 (scale bar=1 µm), (b) Zn(btmbenzene)-3 (scale bar =1 µm), (c) Zn(btmbenzene)-4 (scale bar=30 µm) d) Zn(btmbenzene)-2 after transformation to cubic structures in H_2O/DMF/solvothermal (scale bar=5 µm).

This analysis demonstrated that a major loss of weight occurred at 350 °C that ended at about 420 °C (Fig. S11†). X-ray diffraction (XRD) experiment of the material were carried out to study its structure. According to XRD analysis of microcapsules, the structure is amorphous without any crystalline area (Fig. S9†). Elemental analysis data of the ICPs affirmed $[Zn(btmbenzene)]_n$ for Zn(btmbenzene)-1. Luminescence is a well-known feature of inorganic-organic coordination polymers which is due to the presence of aromatic or conjugated linkers or lanthanide ions in their structures.[16] Photoluminescence characteristics of ICPs were studied by photoluminescence spectroscopy. Excitation of Zn(btmbenzene)-1 microcapsules at 350 nm leaded to emission with peak maximum at 450 nm (Fig. 2b). Fluorescence microscopy images of Zn(btmbenzene)-1 showed an intensive blue emission for these microcapsules (Fig. 2a). Inclusion capability of these self-assembled hollow microspheres was investigated by loading of Rhodamine B fluorescent dye. Rhodamine B is regularly utilized as a tracer dye, hydrophilic model drug and widely in biotechnology applications.[17-19]Therefore, certain amount of the dye was added to the reaction mixture to be entrapped inside the polymeric sphere through an in situ encapsulation process.

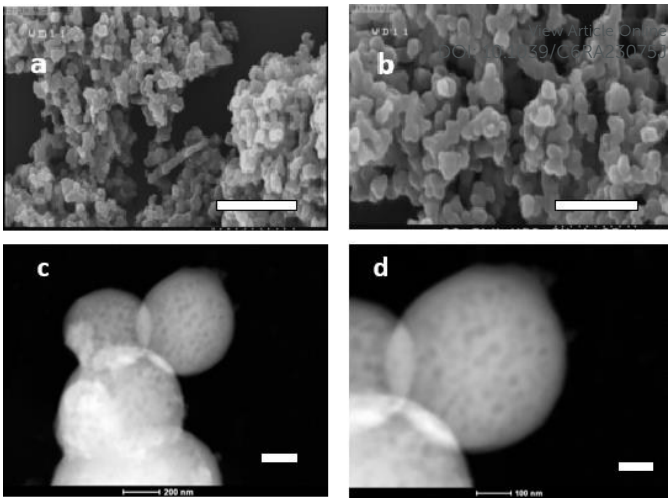

Fig. 5 a, b) SEM images of Fe_3O_4@ Zn(btmbenzene)-2 (scale bar a and b =2 and 1 µm respectively) and c, d) HRTEM images of Fe_3O_4@Zn(btmbenzene)-2 spheres (scale bar c and d =200 and 100 nm respectively)

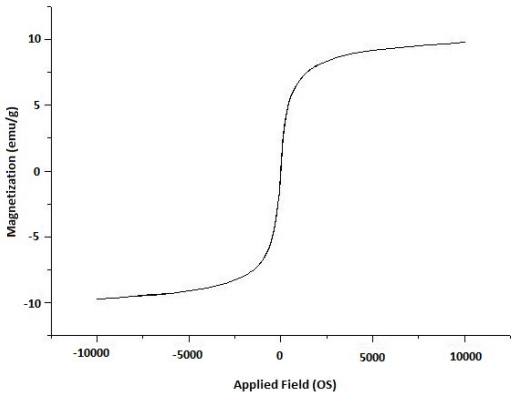

Fig. 6 Magnetic hysteresis loop of Fe_3O_4@ Zn(btmbenzene)-2 measured at room temperature.

Fluorescence optical microscopy and fluorescence spectroscopy analyses were carried out to study the dye inclusion talent of these hollow microspheres. As can be seen in Fig. 3, red emission is associated with excitation upon 540 nm which indicates inclusion of dye molecules into Zn(btmbenzene)-1 named as RhB@Zn(btmbenzene)-1. Quantity of RhB loading into Zn(btmbenzene)-1 was also evaluated by UV-vis spectrophotometer. RhB@Zn(btmbenzene)-1 was dispersed in deionized water at pH of 5 and stirred for 72 h. Next, the mixture was centrifuged and absorbency of the supernatant was determined at 554 nm utilizing UV-vis spectrophotometer. According to UV-vis analysis, loading capacity of Rhodamine B into Zn(btmbenzene)-1 was 20 µmol/g (Table S2 and Fig. S19†). Fig. S20† shows FT-IR spectra of Zn(btmbenzene)-1 and RhB@Zn(btmbenzene)-1 which are the same. Moreover, FESEM image of RhB@Zn(btmbenzene)-1 confirms that the product maintains its spherical morphology after in-situ encapsulation process (Fig. S21†). Therefore, the guest molecules did not interfere the overall synthesis of the host polymer during in-situ encapsulation. Nowadays a common approach for smart drug delivery to tumor cells is applying microcapsules containing human therapeutic drugs.[20-22] 5-Fluorouracil (5-FU) is an anticancer drug which is broadly applied in clinical chemotherapy for the treatment of different tumors as exemplified by breast adenocarcinoma and colon cancer.[23-25]

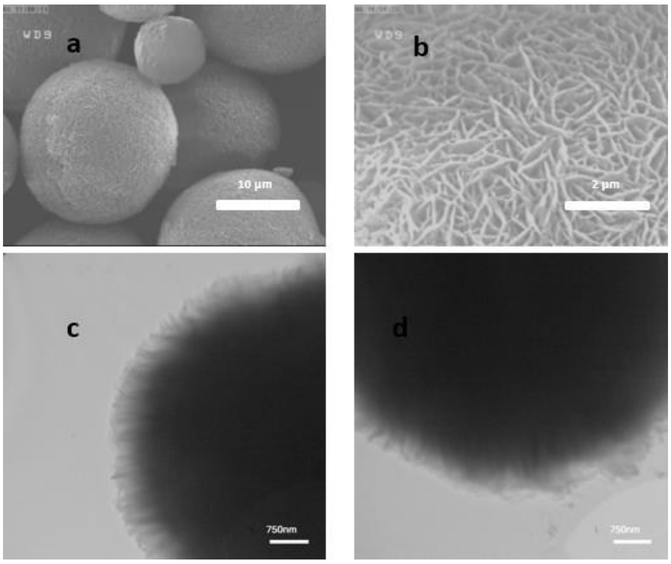

Fig. 7 a) Low-magnification SEM image b) High-magnification SEM images of the Zn(btmbiphenyl)-1 hollow spheres. (c, d) High-resolution TEM image of an individual Zn(btmbiphenyl)-1 sphere.

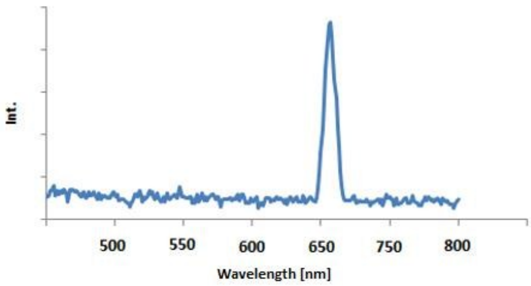

Fig. 8 PL spectrum of Zn(btmbiphenyl)-1 hollow spheres collected at λ_{exc}= 420 nm.

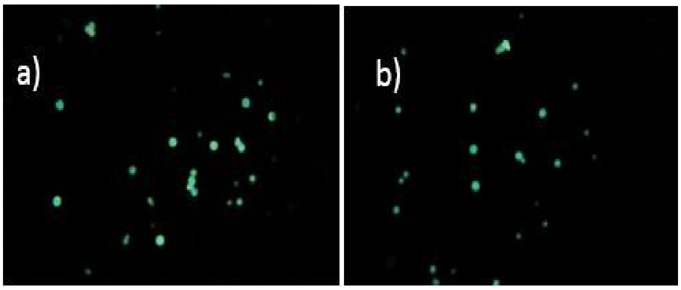

Fig. 9 Fluorescence optical microscopy images of RhB@Zn(btmbiphenyl)-1 (a, b) λ_{exc}= 359 -371 nm and λ_{em}>397 nm.

To exhibit the diversity in ability of these hollow spheres for encapsulation of the molecules, 5-FU was chosen as a guest. Following alike experimental procedure, Zn(btmbenzene)-1 microspheres which entraped 5-FU were synthesized (ESI). 5-FU@Zn(btmbenzene)-1 was dispersed in deionized water at pH of 5 and stirred for 72 h.

UV-vis analysis was performed at 260 nm on the supernatant solution to estimate the quantity of 5-FU loading into 5-FU@Zn(btmbenzene)-1 microspheres. The quantity of 5-FU encapsulation in microspheres was 158 μmol/g. (Table S1 and Fig. S18†). Moreover, influences of different synthesis strategies and solvents on the morphology of this infinite coordination polymer were studied (Scheme 2). Conventional method reported for preparation of metal-organic capsules is fast precipitation referring to addition of a poor solvent to the reaction mixture which leads to precipitation of polymerized hollow metal-organic capsules.[4] Therefore, a solution of $Zn(NO_3)_2{\cdot}6H_2O$ in methanol was added to tetrazolate ligand btmbenzene in DMF under vigorous stirring. Fig. 4a displays the SEM images of the product obtained from the reaction named as Zn(btmbenzene)-2 with the average size of 100 nm. FT-IR spectrum of the sample showed two strong peaks at 1374 and 1667 cm^{-1} similar to Zn(btmbenzene)-1 related to tetrazole coordination to Zn^{2+} ions (Fig. S7†).[26,27] XRD analysis showed an amorphous phase for Zn(btmbenzene)-2 (Fig. S9†). Thermogravimetric analysis of the sample exhibited 20 % weight loss related to DMF and the main weigh loss region is between 320 and 420 °C (Fig. S12†). Fe_3O_4 nanoparticles were selected as a model to investigate the inclusion of the infinite coordination polymers for the insoluble guest. Fe_3O_4 nanoparticles were dispersed in the DMF solution of btmbenzene ligand and methanolic solution of $Zn(NO_3)_2{\cdot}6H_2O$ was added to the mixture gradually (ESI). Fig. 5 demonstrates the corresponding FESEM and TEM images of the product. HRTEM images obviously show Fe_3O_4 nanoparticles entrapped inside the polymeric spheres. The magnetic properties of the obtained Fe_3O_4@ Zn(btmbenzene)-2 capsules were examined utilizing a vibrating sample magnetometer. According to the magnetization curve of the magnetic polymeric nanocapsules, the saturation magnetizations for Fe_3O_4@ Zn(btmbenzene)-2 is 10 emu. g^{-1} (Fig. 6).

In a practice, aqueous solution of zinc nitrate was added to btmbenzene ligand solution in DMF and refluxed for 72 h. Next, the product was separated by centrifuge and characterized by FESEM. FESEM image of this compound named as Zn(btmbenzene)-3 shows the morphology of this coordination polymer is rod like structure (Fig. 4b). XRD analysis of Zn(btmbenzene)-3 rods demonstrated some sharp peaks indicating a semi-crystalline nature (Fig. S9†). Moreover, flower-like structures denominated as Zn(btmbenzene)-4 could be synthesized by reaction of aqueous solution of zinc nitrate and btmbenzene ligand in DMF at 140 °C in a Teflon-lined stainless steel autoclave (Fig. 4c). The structure of the material was studied by XRD analysis which exhibited a crystalline character (Fig. S9†). Elemental analyses were performed for these four morphologies which displayed the same percentages on carbon, nitrogen and hydrogen atoms and approved $[Zn(btmbenzene)]_n$ for all these infinite coordination polymers. As can be seen in Fig. S7, FT-IR spectra of these three morphologies resemble each other with two distinctive strong peaks at about 1400 and 1600 cm^{-1} indicating coordination of tetrazole groups to Zn^{2+} ions. These evidences confirm that all five morphologies of $[Zn(btmbenzene)]_n$ have the same constituents. In addition, transformation of these structures upon changes to exterior circumstances were studied. Zn(btmbenzene)-2 nanocapsules were separated by centrifuge from the reaction mixture and washed with DMF and dried, then put into a Teflon-lined stainless steel autoclave containing DMF and methanol and heated at 120 °C for 24 h. Remarkably, an important morphological transformation occurred and small nanocapsules of Zn(btmbenzene)-2 turned to spherical microcapsules of Zn(btmbenzene)-1 (Fig. S15†). In an experiment, nanocapsules of Zn(btmbenzene)-2 were heated at 140 °C for 72 h in a Teflon-lined stainless steel autoclave containing DMF and H_2O. FESEM images of the product showed that these nanocapsules changed to cubic-like structures (Fig. 4d and S17).

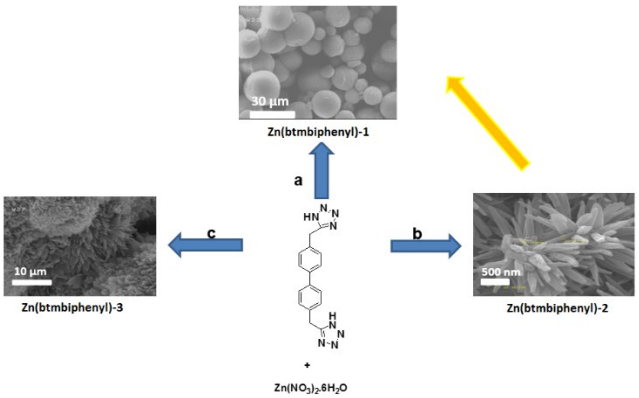

Scheme 3 Synthesis of btmbiphenyl-based nano- and micro-structures: (a) MeOH/DMF/solvothermal conditions (b) MeOH/DMF/fast precipitation method, (c) H_2O/DMF/solvothermal.

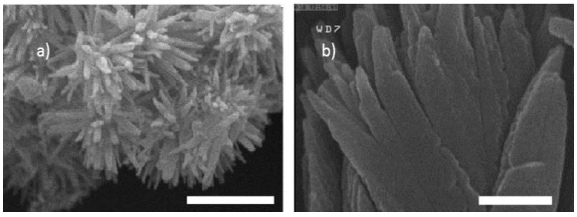

Fig. 10 SEM images of (a) Zn(btmbiphenyl)-2 (scale bar=2 µm), (b) Zn(btmbiphenyl)-3 (scale bar =1 µm).

Zinc oxide nanostructures have been considered as significant key materials due to wide field of applications such as photocatalysts, gas sensors, antimicrobial activities, electronic and optoelectronic devices. Various micro and nanostructures of zinc oxide have been synthesized as exemplified by rods, belts, combs, saws, spirals, rings and hollow spheres.[28-35] Hollow zinc oxide spheres have been considered as an applicable desired morphology of this material due to their special advantages such as good surface area and low density.[36-43] We decided to use these hollow metal-organic microsphere to prepare hollow zinc oxide microspheres through calcination. Therefore, hollow Zn(btmbenzene)-1 spheres were calcinated at 450 and 550 °C for 3 h in the air to find the best temperature to prepare ZnO with retaining the spherical morphology. FESEM images of products show that spheres keep their spherical morphology after calcination at 450 °C but the morphology changed under calcination at 550 °C (Fig. 11). The sample produced at 450 °C was characterized by XRD analysis. Obtained XRD pattern can be indexed to the wurtzite structure of zinc oxide (Fig. S14†). It is noteworthy to mention that any other diffraction peak was not observed confirming the spherical ICPs entirely changed into the ZnO phase. The diversity and development of supramolecular coordination compounds obviously are indebted to the usage of larger extended decorated bridging ligands.[13]We chose a longer linker of the same type (btmbiphenyl) to synthesize an extended network with the morphology of spherical capsule (Scheme 1). To prepare btmbiphenyl ligand, 4,4'-bis(bromomethyl)biphenyl was used as a precursor. The alkyl halide underwent nucleophilic aliphatic substitution with sodium cyanide in distilled H_2O under reflux condition for 24 h. The obtained dinitrile product was transformed into tetrazolate ligand through the reaction with sodium azide and triethylamine hydrochloride under reflux in dry toluene for 72 h and an inert argon atmosphere.

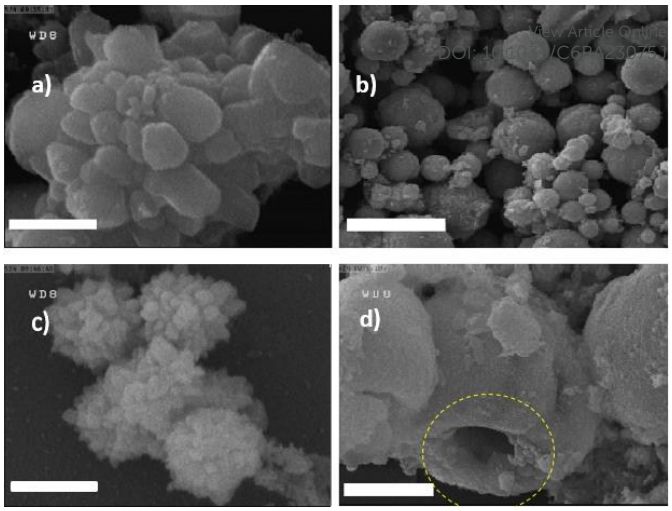

Fig. 11 FESEM images of ZnO architectures obtained from calcination of the prepared ICPs after calcination of (a) Zn(btmbenzene)-1 (scale bar=1 µm), (b) Zn(btmbiphenyl) (scale bar= 20 µm) in air at 550 °C for 3 h, (c) Zn(btmbenzene)-1 (scale bar =1.5 µm) and (d) Zn(btmbiphenyl)-1 (scale bar =5 µm), in air at 450 °C for 3 h.

The work up procedure is accessible in (ESI). Elemental analysis, ^{1}H NMR (Fig. S5†) and ^{13}C NMR (Fig. S6†) spectroscopy proved the synthesis of btmbiphenyl ligand. Following a similar procedure, Zn(btmbiphenyl)-1 microcapsules were prepared by solvothermal reaction of btmbiphenyl ligand in DMF and methanolic solution of $Zn(NO_3)_2{\cdot}6H_2O$ salt in 120 °C. The morphology of as-synthesized product was studied by FESEM analysis. In accordance with the FESEM images (Fig. 7) particles have spherical morphology with average size of 20 µm. As anticipated, by employing the extended linker, the size of the prepared spheres increased obviously. Moreover, unlike Zn(btmbenzene)-1 microcapsules, the surface of these expanded ICPs is completely unsmooth. The structure of Zn(btmbiphenyl)-1 compound was analyzed by HRTEM as well. Fig. 7 exhibits TEM images of the Zn(btmbiphenyl)-1 which validate the formation of hollow microcapsules. Infrared spectrum of the sample resembling that of the material Zn(btmbenzene)-1 reveals frequencies at 1403 and 1604 cm^{-1} proving polymerization of Zn^{2+} ions and tetrazole groups (Fig. S8†). Thermogravimetric study of Zn(btmbiphenyl)-1 exhibited the major weight decline domain between 310 °C and 430 °C relevant to destruction of ICPs (Fig. S13†). Powder x-ray diffraction experiment was carried out to investigate the crystallinity of the sample. Surprisingly, the related XRD pattern displayed sharp peaks indicating the crystalline structure of these capsules (Fig. S10†). The elemental composition of these hollow capsules was examined by elemental analysis. According to elemental analysis $[Zn(btmbiphenyl)]_n$ was offered for Zn(btmbiphenyl)-1. Emission properties of Zn(btmbiphenyl)-1 was studied using photoluminescence spectroscopy. When its microcapsules were excited at 420 nm, the obtained emission spectrum exhibited a peak with λ_{max} at 660 nm (Fig. 8). PL spectrum of Zn(btmbiphenyl)-1 showed an obvious red-shift in comparison with the Zn(btmbenzene)-1. Increasing π-conjugation in the ligand led to a decrease in the HOMO-LUMO gap which caused ligand to metal charge transfer became ineffective and consequently, ligand-based emission occurred and red-shift was observed in the PL spectrum. To investigate the potential of Zn(btmbiphenyl)-1 for loading of 5-FU in a similar procedure, it was encapsulated into the microcapsules (ESI). Amount of 5-FU loaded into the microcapsules was determined utilizing a UV-vis spectrophotometer (Table S1 and

Fig. S18†). Outcomes revealed that the 5-FU loading content was 188 µmol/g which is interestingly more than Zn(btmbenzene)-1. Moreover, encapsulation of Rhodamine B as a guest was performed and analyzed through the identical method (Table S2 and Fig. S19†). According to UV-vis spectrophotometer analysis, Rhodamine B loading capacity of the RhB@Zn(btmbiphenyl)-1 was 25 µmol/g. Fluorescence microscopy images of the RhB@Zn(btmbiphenyl)-1 showed intense green emission related to the encapsulated fluorescent dye (Fig. 9). Fig. S22† displays FT-IR spectra of Zn(btmbiphenyl)-1 and RhB@Zn(btmbiphenyl)-1 which have the same pattern. In addition, FESEM image of RhB@Zn(btmbiphenyl)-1 proves that the sample keeps its spherical morphology after in-situ encapsulation process (Fig. S23†). Therefore, our expectations fulfilled and Zn(btmbiphenyl)-1 microcapsules showed more loading capacity for both 5-FU and Rhodamine B in comparison with Zn(btmbenzene)-1 which can be attributed to stronger host-guest interactions due to additional aromatic ring of btmbiphenyl organic linker (Scheme 1) and larger dimensions of the capsules. Afterward we tried to perform encapsulation of Fe_3O_4 magnetic nanoparticles inside the polymeric spheres through an in situ process by solvothermal method but FESEM analysis of samples did not show any special structure.

Furthermore, the influences of operating conditions and solvents on the morphology of these ICPs were also inspected. To study the conventional method effects on the morphology, methanolic solution of $Zn(NO_3)_2{\cdot}6H_2O$ was added to btmbiphenyl ligand in DMF dropwise at RT under stirring. The separated product was entitled as Zn(btmbiphenyl)-2 and analyzed by FESEM. FESEM images of the Zn(btmbiphenyl)-2 demonstrated that the flower-like structures were synthesized (Fig. 10a). XRD analysis of the sample showed some sharp peaks indicating semi-crystallinity of the compound (Fig. S10†). In next step, aqueous solution of $Zn(NO_3)_2{\cdot}6H_2O$ reacted with btmbiphenyl solution in DMF under solvothermal condition at 140 °C. The morphology of the product named as Zn(btmbiphenyl)-3 was studied by FESEM analysis. As can be seen in Fig. 10b and Scheme 3c flower-like structures were obtained which have much ticker branches in comparison with Zn(btmbiphenyl)-2. The powder was characterized by XRD analysis and indicated that the compound is crystalline (Fig. S10†). FT-IR spectra pattern of Zn(btmbiphenyl)-n (n= 2, 3) appeared like Zn(btmbiphenyl)-1 infrared spectrum (Fig. S8†). According to elemental analyses of Zn(btmbiphenyl)-n (n= 2, 3) these morphologies have the same formula expressed as $[Zn(btmbiphenyl)]_n$ indicating these three morphologies have the similar compositions. Morphological transformation of Zn(btmbiphenyl)-2 under solvothermal condition was also examined. Thereupon, Zn(btmbiphenyl)-2 powder was heated at 120 °C under solvothermal condition in DMF and methanol for 12 h (ESI). Surprisingly, flower-like constructions changed into spherical structures (Fig. S16†). Subsequently, Zn(btmbiphenyl)-1 microcapsules were used to synthesize zinc oxide hollow spheres via calcination. Hence, Zn(btmbiphenyl)-1 microcapsules were heated at 450 and 550 °C for 3h in the air. According to FESEM images of samples shown in Fig. 11 both of the resultant products preserved their spherical morphology. Pursuant to the perforated sphere shown in Fig. 11, emptiness of these structures was also proved even after calcination. The white powder prepared at 450 °C was examined by XRD analysis. The XRD pattern indicated that ZnO with wurtzite structure and hexagonal unit cell was prepared (Fig. S14†). Moreover, determined lattice constants were a= 3.2 and c= 5.2 A°. It is worth noting that the morphology of Zn(btmbenzene)-1 microcapsules and the previously reported Zn(btb)[11] changed after calcination at 550 and 450 °C respectively unlike Zn(btmbiphenyl)-1 microcapsules which could keep the desired hollow spherical morphology in both conditions. Therefore, using Zn(btmbiphenyl)-1 microspheres also seems a better choice for obtaining hollow zinc oxide structures achieving more thermal stability of their morphologies.

Conclusions

In brief, we succeeded to report synthesis of two novel self-assembled hollow spherical metal-organic microcapsules based on two new extended tetrazolate ligands of the same type and Zn^{2+} ions by solvothermal method. Moreover, different morphologies of these ICPs were prepared by changing reaction conditions and solvents which include flower-like structures, cubes and rods. In addition, through an in situ process entrapment of some functional materials such as a kind of anticancer drug, fluorescent dye and inorganic nanoparticles within these coordination networks were examined as a potential application. The loading capacities of these carriers for the examined anticancer drug and fluorescent dye were determined and compared. Furthermore, these spherical polymeric microcapsules were applied as precursors for fabrication of hollow crystalline ZnO spheres via calcination which have been considered as a favorite morphology of zinc oxide due to their potential applications in drug delivery carriers and catalysis.

Acknowledgement

We thank Tarbiat Modares University for supporting of this investigation appreciatively.

References

1 (a) M. Oh and C. A. Mirkin, *Nature*, 2005, **438**, 651; (b) M. Oh and C. A. Mirkin, *Angew. Chem., Int. Ed.*, 2006, **45**, 5492.

2 Y. -M. Jeon, J. Heo and C. A. Mirkin, *J. Am. Chem. Soc.*, 2007, **129**, 7480.

3 (a) H. Maeda, M. Hasegawa, T. Hashimoto, T. Kakimoto, S. Nishio and T. Nakanishi, *J. Am. Chem. Soc.*, 2006, **128**, 10024; (b) X. Sun, S. Dong and E. Wang, *J. Am. Chem. Soc.*, 2005, **127**, 13102; (c) H. Wei, B. Li, Y. Du, S. Dong and E. Wang, *Chem. Mater.*, 2007, **19**, 2987; (d) S. Jung and M. Oh, *Angew. Chem., Int. Ed.*, 2008, **47**, 2049; (e) K. Wang, X. Ma, D. Shao, Z. Geng, Z. Zhang and Z. Wang, *Cryst. Growth Des.*, 2012, **12**, 3786; (f) L. Zhang, X. Gao, L. Yang, P. Yu and L. Mao, *Appl. Mater. Interfaces*, 2013, **5**, 8120; (g) S. Zhong, H. Jing, Y. Li, S. Yin, C. Zeng and L. Wang, *Inorg. Chem.*, 2014, **53**, 8278.

4 I. Imaz, J. Hernando, D. Ruiz-Molina and D. Maspoch, *Angew. Chem., Int. Ed.*, 2009, **48**, 2325.

5 R. Nishiyabu, N. Hashimoto, T. Cho, K. Watanabe, T. Yasunaga, A. Endo, K. Kaneko, T. Niidome, M. Murata, C. Adachi, Y. Katayama, M. Hashizume and N. Kimizuka, *J. Am. Chem. Soc.*, 2009, **131**, 2151.

6 V. Gonzalez, D. A. L. Vignati, C. Leyval and L. Giamberini, *Environ. Int.*, 2014, **71**, 148.

7 N. R. Champness, *Angew. Chem., Int. Ed.*, 2009, **48**, 2274.

8 a) K. Suzuki, J. Lida, S. Sato, M. Kawano and M. Fujita, *Angew. Chem.,* 2008, **120**, 5864; *Angew. Chem., Int. Ed*., 2008, **47**, 5780; b) S. M. Biros, R. M. Yeh and K. N. Raymond, *Angew. Chem.*, 2008, **120**, 6151; *Angew. Chem., Int. Ed*., 2008, **47**, 6062; c) D. J. Tranchemontagne, Z. Ni, M. O· Keeffe and O. M. Yaghi, *Angew. Chem.*, 2008, **120**, 5214; *Angew. Chem., Int. Ed*., 2008, **47**, 5136.

9 X. Zhang, M. A. Ballem, M. Ahre´n, A. Suska, P. Bergman and K. Uvdal, *J. Am. Chem. Soc.*, 2010, **132**, 10391.

10 P. Huang, J. Mao, L. Yang, P. Yu and L. Mao, *Chem. Eur. J.*, 2011, **17**, 11390.

11 Z. Sharifzadeh, S. Abedi and A. Morsali, *J. Mater. Chem. A*, 2014, **2**, 4803.

12 B. Zhang, B. Liu, G. Chen and D. Tang, *Biosens. and Bioelectron.*, 2015, **64**, 6.

13 a) M. Eddaoudi et al. *Science*, 2002, **295**, 469; O. M. Yaghi, M. O'Keeffe, N. W. Ockwig, H. K. Chae, M. Eddaoudi and J. Kim, *Nature*, 2003, **423**, 705; b) H. Furukawa, Y. B. Go, N. Ko, Y. K. Park, F. J. Uribe-Romo, J. Kim, M. O'Keeffe and O. M. Yaghi, *Inorg. Chem*., 2011, **50**, 9147; c) H. C. Zhou , J. R. Long and O. M. Yaghi, *Chem. Rev.,* 2012, **112**, 673; d) A. Schneemann, V. Bon, I. Schwedler, I. Senkovska, S. Kaskel and R. A. Fischer, *Chem. Soc. Rev*., 2014, **43**, 6062.

14 G. Ferey, *Chem. Soc. Rev.*, 2008, **37**, 191.

15 K. Sumida, M. L. Foo, S. Horike and J. R. Long, *Eur. J. Inorg. Chem*., 2010, **24**, 3739.

16 Y. Cui, Y. Yue, G. Qian and B. Chen, *Chem. Rev*., 2012, **112**, 1126.

17 G. Reina, S. Orlanducci, C. Cairone, E. Tamburri, S. Lenti, I. Cianchetta, M. Rossi and M. L. Terranova, *J. Nanosci. Nanotechnol*., 2015, **15**, 1022.

18 K. Gulati, S. Maher, S. Chandrasekaran, D. M. Findlay and D. Losic, *J. Mater. Chem. B*, 2016, **4**, 371.

19 D. Zheng, J. Li, C. Li, Z. Xu, S. X. Cheng and X. Z. Zhang, *J. Mater. Chem. B*, 2015, **3**, 3483.

20 A. P. Esser-Kahn, N. R. Sottos, S. R. White and J. S. Moore, *J. Am. Chem. Soc.*, 2010, **132**, 10266.

21 M. Ambrosi, E. Fratini, P. Baglioni, C. Vannucci, A. Bartolini, A. Pintens, and J. Smets, *J. Phys. Chem. C*, 2016, **120**, 13514.

22 W. Cui, J. Li and G. Decher, *Adv. Mater*., 2016, **28**, 1302.

23 H. Zhao, H. Feng, D. Liu, J. Liu, N. Ji, F. Chen, X. Luo, Y. Zhou, H. Dan, X. Zeng, J. Li, C. Sun, J. Meng, X. Ju, M. Zhou, H. Yang, L. Li, X. Liang, L. Chu, L. Jiang, Y. He and Q. Chen, *ACS Nano,* 2015, **9**, 9638.

24 S. Yu, X. Gao, H. Baigude, X. Hai, R. Zhang, X. Gao, B. Shen, Z. Li, Z. Tan and H. Su, *ACS Appl. Mater. Interfaces*, 2015, **7**, 5089.

25 E. A. K. Nivethaa, S. Dhanavel, V. Narayanan, C. A. Vasu and A. Stephen, *RSC Adv.*, 2015, **5**, 1024.

26 M. Dinca, A. F. Yu and J. R. Long, *J. Am. Chem. Soc.*, 2006, **128**, 17153.

27 S. Jeong, X. Song, S. Jeong, M. Oh, X. Liu, D. Kim, D. Moon and M. S. Lah, *Inorg. Chem.*, 2011, **50**, 12133.

28 T. Guo, M. S. Yao, Y. H. Lin and C. W. Nan, *Cryst. Eng. Comm.*, 2015, **17**, 3551.

29 J. Wang, X. Li, Y. Xia, S. Komarneni, H. Chen, J. Xu, L. Xiang and D. Xie, *ACS Appl. Mater. Interfaces*, 2016, **8**, 8600.

30 S. Park, S. An, H. Ko, Ch. Jin and Ch. Lee, *ACS Appl. Mater. Interfaces*, 2012, **4**, 3650.

31 R. Kumar, S. Anandan, K. Hembram and T. N. Rao, *ACS Appl. Mater. Interfaces*, 2014, **6**, 13138.

32 C. J. Tainter and G. C. Schatz, *J. Phys. Chem. C*, 2016, ***120***, 2950.

33 S. G. Kumar and K. S. R. K. Rao, *RSC Adv.*, 2015, **5**, 3306.

34 L. Wang and M. Muhammed, *J. Mater. Chem.*, 1999, **9**, 2871.

35 L. -Y. Yang, S. -Y. Dong, J. -H. Sun, J.-L. Feng, Q. -H. Wu and S. -P. Sun, *J. Hazard. Mater.,* 2010, **179**, 438.

36 J. Yu and X. Yu, *Environ. Sci. Technol.*, 2008, **42**, 4902.

37 G. Patrinoiu, M. Tudose, J. M. Calderon-Moreno, R. Birjega, P. Budrugeac, R. Ene and O. Carp, *J. Solid State Chem.*, 2012, **186**, 17.

38 K. An and T. Hyeon, *Nano Today*, 2009, **4**, 359.

39 (a) D. M. Vriezema, M. C. Aragon`es, J. A. A. W. Elemans, J. J. L. M. Comelissen, A. E. Rowan and R. J. M. Nolte, *Chem. Rev.*, 2005, **105**, 1445; (b) Y. Zhao and L. Jiang, *Adv. Mater.*, 2009, **21**, 3621.

40 (a) F. Caruso, R. A. Caruso and H. M. Ohwald, *Science*, 1998, **282**, 1111; (b) B. D. G. Geest, N. N. Sanders, G. B. Sukhorukov, J. Demeester and S. C. D. Smedt, *Chem. Soc. Rev.*, 2007, **36**, 636.

41 F. Caruso, *Chem. Eur. J.*, 2000, **6**, 413.

42 X. W. Lou, L. A. Archer and Z. C. Yang, *Adv. Mater.*, 2008, **20**, 3987.

43 L. L. Wang, Z. Lou, T. Fei and T. Zhang, *J. Mater. Chem.*, 2012, **22**, 4767.

View Article Online
DOI: 10.1039/C6RA23075J

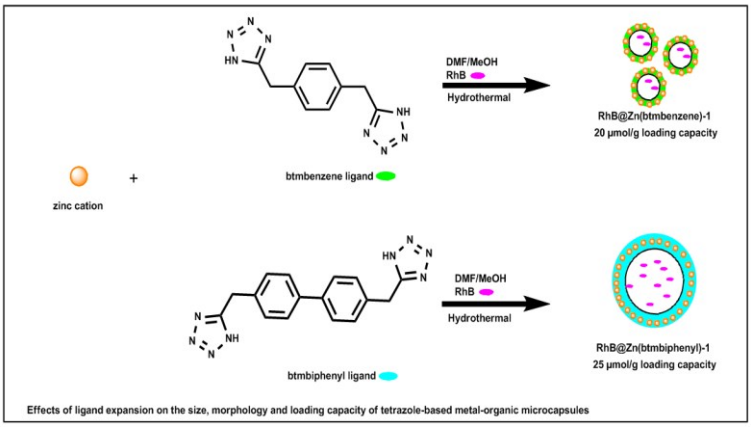

Effects of ligand expansion on the size, morphology and loading capacity of tetrazole-based metal-organic microcapsules